




Quantum theory of feedback cooling of an anelastic macromechanical oscillator

Kentaro Komori ^{1,2,*}, Dominika Ďurovčková ³, and Vivishek Sudhir ^{1,4,†}

¹*LIGO Laboratory, Massachusetts Institute of Technology, Cambridge, Massachusetts 02139, USA*

²*Institute of Space and Astronautical Science, Japan Aerospace Exploration Agency, Sagamihara, Kanagawa 252-5210, Japan*

³*Department of Physics, Massachusetts Institute of Technology, Cambridge, Massachusetts 02139, USA*

⁴*Department of Mechanical Engineering, Massachusetts Institute of Technology, Cambridge, Massachusetts 02139, USA*



(Received 1 November 2021; revised 27 February 2022; accepted 5 April 2022; published 26 April 2022)

Conventional techniques for laser cooling, by coherent scattering off of internal states or through an optical cavity mode, have so far proved inefficient on mechanical oscillators heavier than a few nanograms. That is because larger oscillators vibrate at frequencies much too small compared to the scattering rates achievable by their coupling to auxiliary modes. Decoherence mechanisms typically observed in heavy low-frequency elastically suspended oscillators also differ markedly from what is assumed in conventional treatments of laser cooling. We show that for a low-frequency anelastic oscillator forming the mechanically compliant end mirror of a cavity, detuned optical readout, together with measurement-based feedback to stiffen and dampen it, can harness ponderomotively generated quantum correlations to realize efficient cooling to the motional ground state. This will pave the way for experiments that call for milligram-scale mechanical oscillators prepared in pure motional states, for example, for tests of gravity’s effect on massive quantum systems.

DOI: [10.1103/PhysRevA.105.043520](https://doi.org/10.1103/PhysRevA.105.043520)

I. INTRODUCTION

The purity with which quantum states of tangibly massive objects can be prepared remains an open experimental challenge [1–3]. Although workers in the fields of atomic physics [4–9], and more recently cavity optomechanics [10–18], have succeeded in addressing this challenge at subnanogram mass scales, objects with a significantly larger mass feature a qualitatively different behavior. The central pathology remains the same, namely, decoherence, but the precise symptom is unique at large masses.

Small-mass objects, elastically or electromagnetically bound, can be taken to be a mechanical oscillator that is subject to a viscous damping force proportional to its velocity (called velocity damping). For trapped atoms, this is due to the fact that there is little internal dissipation, and any external dissipation arises predominantly from background gas collisions, which are naturally described through impulsive momentum kicks; the fluctuation-dissipation theorem then assigns a velocity-damped model for motional decoherence. Levitated nanomechanical systems, recently prepared in their motional ground state [15,16], appear to be immune to internal dissipation, despite large internal temperatures [19], apparently due to negligible coupling between internal modes and center-of-mass motion. Nanomechanical objects are elastically bound so as to realize radio-frequency mechanical oscillators; the effects of internal dissipation are largely masked at such high frequencies [20]. The upshot is that all existing theoretical consideration of laser cooling of

mechanical oscillators implicitly assumes a velocity-damped oscillator [21–32].

Large-mass objects have been isolated so as to be largely immune to external damping. To wit, gas damping scales inversely with the mass [33–35], while suspension techniques have been developed (such as that employed in LIGO) that are not limited by loss to an external agency. Internal damping dominates their decoherence. A most ubiquitous form of internal damping in elastic oscillators is anelasticity [20,36,37], for which the damping is not velocity proportional, but is described by a frequency-dependent “structural damping” rate, $\Gamma_0[\Omega] = (\Omega_0/Q_0)(\Omega_0/\Omega)$, where Ω_0 is the resonance frequency, and Q_0 is the (frequency-independent) quality factor.

The decoherence rate of a structurally damped oscillator, when exposed to a thermal bath of mean occupation $n_{\text{th}}[\Omega] \approx k_B T / \hbar \Omega$,

$$\Gamma_{\text{th}}[\Omega] = n_{\text{th}}[\Omega] \Gamma_0[\Omega] \approx \frac{k_B T}{\hbar Q_0} \left(\frac{\Omega_0}{\Omega} \right)^2,$$

decreases quadratically with frequency, in marked contrast to a velocity-damped oscillator (for which the scaling is linear). This can be harnessed by stiffening the oscillator—for example, by radiation pressure forces from a cavity field [38–40]—so as to establish an oscillator mode at the frequency $\Omega_{\text{eff}} \gg \Omega_0$, whose thermal decoherence rate, $\Gamma_{\text{th}}[\Omega_{\text{eff}}] = \Gamma_{\text{th}}[\Omega_0](\Omega_0/\Omega_{\text{eff}})^2$, can be significantly lower than that of the intrinsic mode (at frequency Ω_0). However, this will be counteracted by additional decoherence from quantum fluctuations of the optical field used to produce the optical spring. The interplay of these two effects, given the scaling of the decoherence rate for a structurally damped oscillator, calls for a reexamination of the conventional theory of laser cooling [21–23,25] as applied to macroscopic

*komori.kentaro@jaxa.jp

†vivishek@mit.edu

mechanical oscillators. As we will show, this naturally brings up the opportunity to consider improvement of the cooling performance through back-action evasion.

In the following we study laser cooling of structurally damped and optically stiffened mechanical oscillators via their coupling to an optical cavity field. Because typical macroscopic mechanical oscillators coupled to optical cavities tend to be in the broadband cavity regime (i.e., mechanical frequency much lower than the cavity decay rate), cooling from cavity dynamical back-action is not practical to realize pure quantum states, so we consider active feedback based on cavity-enhanced measurement of the oscillator position as the cooling mechanism [14,21,25,41]. In fact, significant optical stiffening, by blue-detuning the cavity mode it is coupled to, requires external feedback to stabilize the oscillator against parametric instabilities [42]. The natural rotation of the field quadratures due to cavity detuning, possibly enhanced by choice of homodyne measurement angle to derive the error signal for feedback, gives rise to the possibility of enhancing the performance of feedback cooling using quantum correlations developed intrinsically in the radiation-pressure interaction [43].

II. FEEDBACK COOLING WITH ACTIVE AND DETUNED OPTICAL SPRING

We consider here the following scenario [depicted in Fig. 1(a)]: A mechanical oscillator, with displacement fluctuations δx , forms the end mirror of an optical cavity, whose motion modulates the cavity frequency as $G \cdot \delta x$; the cavity is probed by an ideal coherent field detuned from resonance by Δ , and is otherwise lossless; the reflected light is subjected to homodyne detection with a local oscillator whose phase differs from that of the cavity input by θ ; and the resulting photocurrent fluctuations are passed through a causal filter to synthesize a force—the feedback force—that impresses upon the oscillator. Despite the complexity of the scenario, the motion of the oscillator can be described by a simple linear equation (in the frequency domain),

$$\chi_0^{-1}[\Omega]\delta x[\Omega] = \delta F_{\text{th}}[\Omega] + F_{\text{rp}}[\Omega] + F_{\text{fb}}[\Omega]. \quad (1)$$

It describes the intrinsic response,

$$\chi_0[\Omega] = [m(-\Omega^2 + \Omega_0^2 + i\Omega\Gamma_0[\Omega])]^{-1}, \quad (2)$$

of the oscillator—with mass m , intrinsic resonance frequency Ω_0 , and damping $\Gamma_0[\Omega]$ —to three forces.

A. Structural thermal force

The thermal force δF_{th} is characterized by its (symmetrized double-sided) spectral density,

$$\bar{S}_{FF}^{\text{th}}[\Omega] = 2\hbar(n_{\text{th}}[\Omega] + \frac{1}{2})m\Omega\Gamma_0[\Omega], \quad (3)$$

where $n_{\text{th}}[\Omega] \approx kT/(\hbar\Omega)$ is the average thermal phonon occupation. Note that structural thermal force decreases with frequency [i.e., $\bar{S}_{FF}^{\text{th}}[\Omega] \approx 2\hbar m \Omega \Gamma_{\text{th}}[\Omega] \propto 1/\Omega$]—in contrast to velocity-damping which is frequency-independent—which implies that the resulting thermal displacement spectrum scales as Ω^{-5} for frequencies above resonance [see Fig. 1(b)].

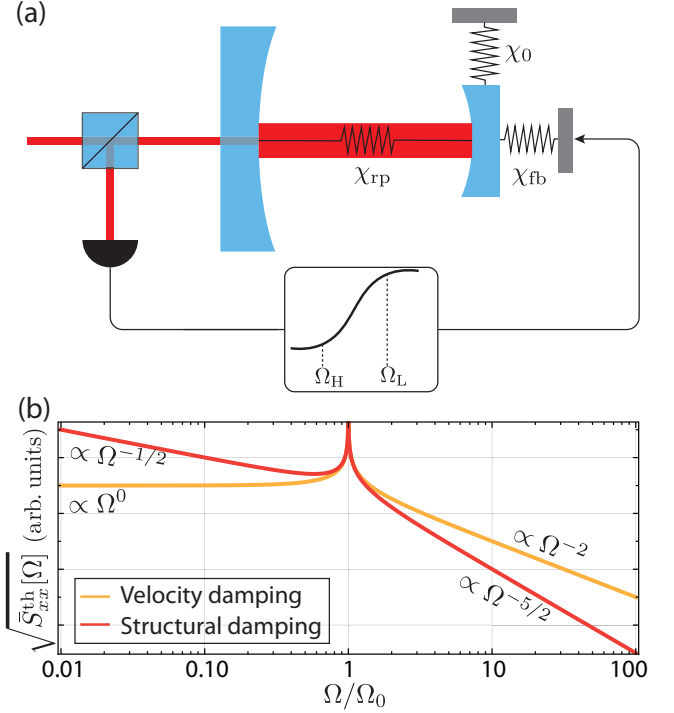


FIG. 1. (a) A schematic picture of our model of feedback cooling. A mechanical oscillator with intrinsic susceptibility χ_0 is trapped by two additional springs—one induced by optical radiation pressure (χ_{rp}) and another induced by measurement-based feedback (χ_{fb})—so that the effective resonant frequency is significantly increased. The feedback filter is characterized by two cutoff frequencies $\Omega_{\text{H,L}}$ that define the mechanical mode of interest. (b) Displacement fluctuations of a structurally damped (red) and velocity-damped (yellow) oscillator, showing the stronger decrease of structural thermal noise at frequencies above resonance.

B. Radiation pressure force: Optical trapping versus quantum back-action

The radiation pressure force $F_{\text{rp}}[\Omega]$ arises from an interaction between the oscillator displacement and intracavity field (a) described by the interaction Hamiltonian [44], $H_{\text{rp}} = -\hbar G n x$, where $n = a^\dagger a$ is the intracavity photon number. In a linearized description, the radiation pressure force can be expressed as the sum of two components [45],

$$F_{\text{rp}}[\Omega] = -\chi_{\text{rp}}^{-1}[\Omega]\delta x[\Omega] + \delta F_{\text{rp}}[\Omega]. \quad (4)$$

The first is a detuning-dependent force that is proportional to the oscillator position, and leads to optical damping and/or antidamping and spring shift, while the second is a quantum radiation pressure force fluctuation due to intracavity photon number fluctuations. In the broadband cavity regime [i.e., where the cavity decay rate (κ) is much larger than the mechanical frequency] the former is described by a susceptibility of the form

$$\chi_{\text{rp}}^{-1} = m(\Omega_{\text{rp}}^2 + i\Omega\Gamma_{\text{rp}}), \quad (5)$$

where

$$\Omega_{\text{rp}}^2 \approx \Omega_{\text{SQL}}^2 \frac{\delta}{2(1 + \delta^2)}, \quad \Gamma_{\text{rp}} \approx -\frac{\Omega_{\text{SQL}}^2}{\kappa} \frac{2\delta}{(1 + \delta^2)^2}, \quad (6)$$

are the shifts in the oscillator frequency and damping rate due to the radiation pressure interaction. Here, $\delta = \Delta/(\kappa/2)$ is the detuning normalized to the cavity's full width at half maximum (FWHM), n_c is the mean intracavity photon number, and we have defined

$$\Omega_{\text{SQL}} = \sqrt{\frac{8\hbar G^2 n_c}{m\kappa}}, \quad (7)$$

the frequency at which the free-mass standard quantum limit (SQL) is attained.

Note that, in the theory of cavity optomechanics applied to high-frequency oscillators, the radiation-pressure-induced change in the oscillator frequency is typically small compared to the intrinsic resonance frequency (i.e., $\Omega_{\text{rp}} \ll \Omega_0$). In that case, the characteristic interaction frequency is the vacuum optomechanical coupling rate, $G\sqrt{n_c}\sqrt{\hbar/(2m\Omega_0)}$, defined with respect to the zero-point motion of the intrinsic oscillator at frequency Ω_0 . In contrast, here we consider the scenario where the optical spring frequency can be much larger than the intrinsic frequency (i.e., $\Omega_{\text{rp}} \gg \Omega_0$), and we are interested in the properties of the oscillator mode established at the shifted frequency. Achieving this scenario gives the advantage of the frequency dependence in the structural damping. Even when the shifted mechanical frequency is much different from its intrinsic frequency, the trade-off between measurement sensitivity and back-action force remains constrained by fundamental constants (explicated below). Thus, in the terminology of imprecision and back-action noises (see below), the SQL frequency, implicitly defined by $(m\Omega_{\text{SQL}})^2 \bar{S}_{xx}^{\text{imp}}[\Omega_{\text{SQL}}] = \bar{S}_{FF}^{\text{rp}}[\Omega_{\text{SQL}}]$, is a more convenient measure of the interaction strength that is independent of the mechanical resonance frequency. Note that this implicit definition clarifies the interpretation that it is the frequency at which the SQL is achieved. When both the imprecision and back-action noises are white, for example, for displacement readout using a broadband cavity, explicit expressions for these noises give the form in Eq. (7). The implicit definition is, however, valid more generally.

The effect of the position-dependent term in the radiation pressure force [first term in Eq. (4)] is to change the effective response of the oscillator. Indeed, inserting the form of the radiation-pressure-modified response [Eq. (5)] in Eq. (1) and rearranging terms shows that the radiation-pressure-modified response,

$$\begin{aligned} (\chi_0^{-1} + \chi_{\text{rp}}^{-1})^{-1} \approx & [m(-\Omega^2 + (\Omega_0^2 + \Omega_{\text{rp}}^2) \\ & + i\Omega(\Gamma_0 + \Gamma_{\text{rp}}))]^{-1}, \end{aligned}$$

features a mechanical oscillator at a higher frequency ($\Omega_0^2 + \Omega_{\text{rp}}^2$)^{1/2} $\gg \Omega_0$ for blue-detuned (i.e., $\delta > 0$) operation. Since the thermal force decreases with frequency, the displacement fluctuations due to thermal noise at Ω_{rp} can be lower than that at the oscillator's intrinsic resonance frequency Ω_0 .

Two effects, however, affect this conclusion. First, quantum fluctuations in the intracavity photon number, due to the blue-detuned light used to stiffen the oscillator, create an additional radiation pressure force fluctuation (see Appendix A),

$\bar{S}_{FF}^{\text{rp}} = (\hbar G)^2 \bar{S}_{nn} \approx 4\hbar(\hbar G^2 n_c/\kappa)/(1 + \delta^2)$, or equivalently,

$$\bar{S}_{FF}^{\text{rp}}[\omega] = \hbar \frac{m\Omega_{\text{SQL}}^2}{2(1 + \delta^2)} = \hbar \frac{m\Omega_{\text{rp}}^2}{\delta} \Big|_{\delta > 0}. \quad (8)$$

Note that this quantum back-action noise increases quadratically with the stiffened oscillator frequency (for fixed detuning and increasing laser power). The second problem is that as the blue-detuned optical power is increased to realize a stiffer trap for the oscillator, the total damping rate can become negative (i.e., $\Gamma_0 + \Gamma_{\text{rp}} < 0$), causing the oscillator motion to get amplified, and the optomechanical system becomes unstable or nonlinear.

Both these problems—increased quantum back-action with oscillator frequency, and instability—can be controlled by applying a feedback force on the oscillator based on an estimate of its position. The nature of the feedback, to be discussed in Sec. II D, is such that the oscillator motion is simultaneously damped with an amplitude smaller than the ambient thermal motion, where we expect the resulting dynamics to be linear. (In an actual experiment, the trapping field and feedback damping will need to be energized simultaneously.)

C. Displacement measurement: Imprecision, back-action, and back-action evasion

The optical field used to pump the cavity—the same one that when detuned produces the optical spring—is modulated by the motion of the mechanical oscillator. Measuring the quadratures of the field leaking out of the cavity, for example, by homodyne detection, realizes a linear measurement of the mechanical oscillator's displacement. The homodyne photocurrent, appropriately normalized, produces a linear estimate of the position,

$$\delta x_{\text{obs}}[\Omega] = \delta x[\Omega] + \delta x_{\text{imp}}[\Omega], \quad (9)$$

contaminated by the displacement-equivalent imprecision noise δx_{imp} , due to shot-noise fluctuations of the field quadrature that is detected. Since the back-action force δF_{rp} also arises from the vacuum fluctuations of the same field, the imprecision and back-action satisfy two constraints (see Appendix A),

$$\bar{S}_{FF}^{\text{rp}}[\Omega] \bar{S}_{xx}^{\text{imp}}[\Omega] = \frac{\hbar^2}{4\eta} \csc^2 \theta_{\text{eff}}, \quad (10)$$

$$\bar{S}_{Fx}^{\text{rp,imp}}[\Omega] = -\frac{\hbar}{2\sqrt{\eta}} \cot \theta_{\text{eff}}, \quad (11)$$

where

$$\theta_{\text{eff}} = \theta - \tan^{-1} \delta \quad (12)$$

is the effective quadrature angle of the reflected light that is measured (for example, using a homodyne detector), and η is the detection efficiency. The first expresses the essence of the uncertainty principle: the measurement imprecision and back-action force are a mutual trade-off. The conventional measurement strategy—for phase quadrature homodyne readout of the reflection ($\theta_{\text{eff}} = \pi/2$)—can realize a quantum-ideal measurement (i.e., $\bar{S}_{FF}^{\text{rp}} \bar{S}_{xx}^{\text{imp}} = \hbar^2/4$) if the detection efficiency is unity. The second expression relays the fact that the back-action force and imprecision noise can be correlated—but only for finite detuning and/or homodyne

readout of nonphase quadratures—due to the fact that traces of the same optical field fluctuations that produce the back-action force manifest also in the imprecision noise. When these are anticorrelated (i.e., $\bar{S}_{F_x}^{\text{rp,imp}} < 0$), the detected field quadrature can be squeezed, and (some of) the back-action of the measurement avoided. Eqs. 10 and 11 exhaustively characterize the constraints on the measurement due to quantum mechanics at the level of spectral densities; in fact they verify the generalized uncertainty principle, $\bar{S}_{F_x}^{\text{rp}} \bar{S}_{x_x}^{\text{imp}} - |\bar{S}_{F_x}^{\text{rp,imp}}|^2 = \hbar^2/4$ [46,47].

D. Feedback force: Active spring and damping versus feedback back-action

Finally, a feedback force can be applied on the mechanical oscillator, based on such a measurement, i.e.,

$$F_{\text{fb}}[\Omega] = -\chi_{\text{fb}}[\Omega]\delta x_{\text{obs}}[\Omega], \quad (13)$$

where $\chi_{\text{fb}}[\Omega]$ is a causal function chosen to produce the desired modification of the oscillator's effective response. (In principle there could be an additional force noise associated with the feedback force—for example, from the actuator in the feedback path, or technical noises in the photocurrent inside the passband of χ_{fb}^{-1} —but this can always be made negligible as long as a sufficiently high-power quantum-noise-limited local oscillator is used in the homodyne detector. In this case, the homodyne detector acts as a high-gain phase-sensitive amplifier, and so the quantum noise of the optical field, assimilated into δx_{imp} , is the only relevant noise.) Inserting Eqs. (4) and (13) in Eq. (1) produces the equation of motion modified by radiation pressure and feedback:

$$\chi_{\text{eff}}^{-1}[\Omega]\delta x[\Omega] = \delta F_{\text{th}}[\Omega] + \delta F_{\text{rp}}[\Omega] - \chi_{\text{fb}}^{-1}\delta x_{\text{imp}}[\Omega], \quad (14)$$

where $\chi_{\text{eff}}[\Omega]$ is the effective response given by

$$\chi_{\text{eff}}^{-1} = \chi_0^{-1} + \chi_{\text{rp}}^{-1} + \chi_{\text{fb}}^{-1}. \quad (15)$$

In order to affect active spring stiffening and cooling, the feedback susceptibility needs to approximate the form,

$$\chi_{\text{fb}}^{-1} = m(\Omega_{\text{fb}}^2 + i\Omega\Gamma_{\text{fb}}), \quad (16)$$

around the oscillator's stiffened frequency; here $\Omega_{\text{fb}}, \Gamma_{\text{fb}} > 0$. This form is comparable to the radiation-pressure-induced susceptibility in Eq. (5). The effective susceptibility then takes the form

$$\chi_{\text{eff}}^{-1} = m(-\Omega^2 + \Omega_{\text{eff}}^2 + i\Omega\Gamma_{\text{eff}}), \quad (17)$$

which is the response of an oscillator at the shifted frequency, $\Omega_{\text{eff}} = \Omega_0 + \Omega_{\text{rp}} + \Omega_{\text{fb}}$, with a modified damping rate, $\Gamma_{\text{eff}}[\Omega] = \Gamma_0[\Omega] + \Gamma_{\text{rp}} + \Gamma_{\text{fb}}$.

The displacement spectrum of the oscillator so realized takes the form

$$\begin{aligned} \bar{S}_{x_x}[\Omega] &= |\chi_{\text{eff}}[\Omega]|^2 (\bar{S}_{F_x}^{\text{th}}[\Omega] + \bar{S}_{F_x}^{\text{rp}}[\Omega] + |\chi_{\text{fb}}[\Omega]|^{-2} \bar{S}_{x_x}^{\text{imp}}[\Omega] \\ &\quad + 2\text{Re}(\chi_{\text{fb}}^{-1}[-\Omega] \bar{S}_{F_x}^{\text{rp,imp}}[\Omega])). \end{aligned} \quad (18)$$

Here the first line represents the physical motion of the oscillator due to the thermal, radiation pressure back-action, and “feedback back-action” forces; the latter is due to imprecision noise fed back as a force through the filter χ_{fb}^{-1} . The second term is due to imprecision-back-action correlations arising from detuning of the cavity from resonance, or detuning of the homodyne detector from phase quadrature.

E. Feedback filter for ground-state cooling

When the objective is to cool the mechanical oscillator, a convenient figure of merit is the average phonon number, n_{eff} , defined through the average energy,

$$\frac{\langle \delta p^2 \rangle}{2m} + \frac{m\Omega_{\text{eff}}^2 \langle \delta x^2 \rangle}{2} \equiv \hbar\Omega_{\text{eff}} \left(n_{\text{eff}} + \frac{1}{2} \right).$$

Here δp is the fluctuation in the momentum of the oscillator, which is unobserved. However, it can be estimated from the observed displacement as $\delta p[\Omega] = -im\Omega \delta x[\Omega]$, so that the required variances $\langle \delta x^2 \rangle$, $\langle \delta p^2 \rangle$ can be inferred from the spectral density \bar{S}_{x_x} alone as

$$\langle \delta x^2 \rangle = \int_{-\infty}^{\infty} \frac{d\Omega}{2\pi} \bar{S}_{x_x}[\Omega], \quad \langle \delta p^2 \rangle = \int_{-\infty}^{\infty} \frac{d\Omega}{2\pi} (m\Omega)^2 \bar{S}_{x_x}[\Omega]. \quad (19)$$

Mathematically carrying out this program to estimate the phonon number for a structurally damped oscillator that is controlled with the feedback filter in Eq. (16) turns out to be impossible. This is for two reasons:

(1) At low frequencies, even without feedback, the variance in the displacement of a structurally damped oscillator is formally infinite [36]. The physical reason is that structural damping, just like any physical process dominated by $1/f$ noise, is due to nonequilibrium processes at slower and slower time scales [48–50], which precludes thermal equilibrium.

(2) At high frequencies, feedback of imprecision noise as a force noise leads to a formally infinite momentum [51]. This can be seen as follows: When Eq. (18) is used to estimate the momentum variance as the integral of $(m\Omega)^2 \bar{S}_{x_x}$, the term in the integral proportional to the imprecision noise, $\Omega^2 |\chi_{\text{eff}}|^2 |\chi_{\text{fb}}|^{-2} \bar{S}_{x_x}^{\text{imp}}$, is a constant at high frequencies, since $|\chi_{\text{eff}}[\Omega \gg \Omega_{\text{eff}}]|^2 \sim \Omega^{-4}$, while $|\chi_{\text{fb}}[\Omega \gg \Omega_{\text{eff}}]|^{-2} \sim \Omega^2$, and (at best) $\bar{S}_{x_x}^{\text{imp}}$ is frequency independent.

In other words, a structurally damped oscillator does not strictly satisfy the equipartition principle; naive feedback compounds the problem.

In practice, all experiments have a finite bandwidth and observation time which regulates the singularities at high and low frequencies, respectively. In particular, for a large spring ($\Omega_{\text{eff}} \gg \Omega_0$) the effect of structural damping can be well approximated by taking the damping rate to be constant around resonance, i.e., $\Gamma_0[\Omega] \approx \Gamma_0[\Omega_{\text{eff}}] = \Omega_0^2 / (Q_0 \Omega_{\text{eff}})$. To regulate the problem with the momentum variance, we modify the feedback filter to the form

$$\chi_{\text{fb}}^{-1}[\Omega] = m\Omega_0^2 \frac{1 + i\Omega/\Omega_{\text{H}}}{1 + i\Omega/\Omega_{\text{L}}} g_{\text{fb}}, \quad (20)$$

where Ω_{H} and Ω_{L} are high- and low-pass frequencies between which feedback is active ($\Omega_{\text{L}} > \Omega_{\text{H}}$), and $g_{\text{fb}} > 0$ is the dimensionless gain. In this case, unlike the naive filter in Eq. (16), we have that $|\chi_{\text{fb}}[\Omega \gg \Omega_{\text{eff}}]|^{-2} \sim m\Omega_0^2 g_{\text{fb}}^2$, so that $\Omega^2 |\chi_{\text{eff}}|^2 |\chi_{\text{fb}}|^{-2} \bar{S}_{x_x}^{\text{imp}} \sim \Omega^{-2}$, which regulates the high-frequency divergence of the momentum integral. However, in order to realize a spring and damping, the filter in Eq. (20)

must conform to the form in Eq. (16) at some frequencies; indeed we have

$$\chi_{\text{fb}}^{-1}[\Omega \ll \Omega_L] \approx m\Omega_0^2 \left(1 + i \frac{\Omega}{\Omega_H}\right) g_{\text{fb}}.$$

Comparing this with Eq. (16) implies that the feedback damping is $\Gamma_{\text{fb}} = g_{\text{fb}}\Omega_0^2/\Omega_H$, and the spring shift is $\Omega_{\text{fb}} = \sqrt{g_{\text{fb}}\Omega_0^2} = \sqrt{\Omega_H\Gamma_{\text{fb}}}$.

$$2n_{\text{eff}} + 1 = \left[\frac{2\Omega_{\text{eff}}^2 + (\Omega_L - \Omega_H)\Gamma_{\text{eff}} + 2\Omega_L^2}{\Omega_L^2} \left(n_{\text{th,eff}} + n_{\text{ba}} + \frac{1}{2} \right) \frac{\Gamma_0[\Omega_{\text{eff}}]}{\Gamma_{\text{eff}}} + \frac{2\Omega_{\text{eff}}^2 + (\Omega_L - \Omega_H)\Gamma_{\text{eff}} + 2\Omega_H^2}{\Omega_{\text{eff}}^2} n_{\text{imp}} \frac{\Gamma_{\text{eff}}}{\Gamma_0[\Omega_{\text{eff}}]} - \frac{2\Omega_{\text{eff}}^2 + (\Omega_L - \Omega_H)\Gamma_{\text{eff}} + 2\Omega_L\Omega_H}{\Omega_L\Omega_{\text{eff}}} n_{\text{cor}} \right] \left(1 - \frac{\Omega_H}{\Omega_L}\right)^{-1}. \quad (21)$$

Here, $n_{\text{th,eff}} = n_{\text{th}}[\Omega_{\text{eff}}] = n_{\text{th}}[\Omega_0](\Omega_0/\Omega_{\text{eff}})$ is the average phonon occupation of the stiffened oscillator, $n_{\text{ba}} = n_{\text{th,eff}} \cdot \bar{S}_{FF}^{\text{ip}}/\bar{S}_{FF}^{\text{th}}[\Omega_{\text{eff}}]$ is the average phonon occupation due to quantum back-action, n_{imp} is the phonon-equivalent imprecision noise defined through the uncertainty relation [Eq. (10)], $n_{\text{imp}}n_{\text{ba}} = (16\eta)^{-1} \text{csc}^2 \theta_{\text{eff}}$, and $n_{\text{cor}} = (2\sqrt{\eta})^{-1} \cot \theta_{\text{eff}}$ is the phonon-equivalent correlation between imprecision and back-action.

III. DISCUSSION

The first and second terms in Eq. (21) denote the feedback suppression of the total energy of the stiffened oscillator ($\propto n_{\text{th,eff}} + n_{\text{ba}}$) and the heating due to feedback injection of imprecision noise, respectively. The third term, negative in contribution, is the effect of back-action cancellation originating from imprecision-back-action correlations developed through the radiation pressure interaction [52–54]. Such quantum correlations can be harnessed when feedback is predicated on readout of the outgoing field's quadrature that is away from phase quadrature (as shown in Ref. [43] for feedback damping with resonant cavity readout for a velocity-damped oscillator).

A. Conventional case: Feedback with resonant phase-quadrature readout

Before delving into further discussion, note first that the practice of estimating the phonon occupation by assuming the equipartition principle, i.e., taking $2n_{\text{eff}} + 1 = (2m\Omega_{\text{eff}}/\hbar)\langle \delta x^2 \rangle$, is equivalent to taking the low-pass cutoff to be $\Omega_L \rightarrow \infty$; in this case, Eq. (21) reduces to

$$n_{\text{eff}} + \frac{1}{2} \approx \left(n_{\text{th,eff}} + n_{\text{ba}} + \frac{1}{2} \right) \frac{\Gamma_0[\Omega_{\text{eff}}]}{\Gamma_{\text{eff}}} + \left(1 + \frac{\Omega_H^2}{\Omega_{\text{eff}}^2} \right) n_{\text{imp}} \frac{\Gamma_{\text{eff}}}{\Gamma_0[\Omega_{\text{eff}}]} - \frac{\Omega_H}{\Omega_{\text{eff}}} n_{\text{cor}}.$$

For phase measurement at zero detuning (i.e., $\theta_{\text{eff}} = \pi/2$, $\delta = 0$), the effective resonance frequency is $\Omega_{\text{eff}}^2 \approx \omega_h \Gamma_{\text{eff}}$, so that

An additional complication of this choice of the feedback filter is that it need not render the system unconditionally stable in the presence of radiation pressure back-action. A simple Routh-Hurwitz analysis of the effective susceptibility χ_{eff} shows that the system is stable if $g_{\text{fb}} > -\Gamma_{\text{rp}}\Omega_L\Omega_H/[\Omega_0^2(\Omega_L - \Omega_H)]$. We assume that sufficient feedback damping can be realized to satisfy this condition.

With these issues addressed, the oscillator's mean phonon number can be computed from the displacement spectral density. The result can be expressed in closed form (see Appendix B):

the above expression can be cast as

$$n_{\text{eff}} + \frac{1}{2} \approx \left[n_{\text{th,eff}} + n_{\text{ba}} + \frac{1}{2} + \left(\frac{\Omega_{\text{eff}}}{\Gamma_0[\Omega_{\text{eff}}]} \right)^2 n_{\text{imp}} \right] \frac{\Gamma_0[\Omega_{\text{eff}}]}{\Gamma_{\text{eff}}} + n_{\text{imp}} \frac{\Gamma_{\text{eff}}}{\Gamma_0[\Omega_{\text{eff}}]}, \quad (22)$$

consistent with the experiments on feedback cooling of a structurally damped actively stiffened oscillator near its ground state [1].

The case of no active spring corresponds to setting $\Omega_{\text{eff}} = 0$ (because we have assumed that $\Omega_{\text{eff}} \gg \Omega_0$ in the above equation). With resonant readout, there is no additional source of spring stiffening either. In this case, the above equation reduces to $(n_{\text{eff}} + \frac{1}{2})\Gamma_{\text{eff}} \approx (n_{\text{th}} + n_{\text{ba}} + \frac{1}{2})\Gamma_0 + n_{\text{imp}}\Gamma_{\text{eff}}$, which can be interpreted as a detailed balance relation describing a velocity-damped oscillator simultaneously coupled to its thermal and back-action baths at rate Γ_0 , and via feedback to the bath due to measurement imprecision at rate Γ_{eff} . Optimizing over the damping rate shows that $n_{\text{eff}} + \frac{1}{2} \gtrsim 2\sqrt{(n_{\text{th}} + n_{\text{ba}} + \frac{1}{2})n_{\text{imp}}}$; using the uncertainty relation, $n_{\text{imp}}n_{\text{ba}} \geq \frac{1}{16}$ further gives $n_{\text{eff}} + \frac{1}{2} \gtrsim 2\sqrt{(n_{\text{th}} + \frac{1}{2})n_{\text{imp}} + \frac{1}{16}}$. Thus, to realize $n_{\text{eff}} < 1$ requires that $n_{\text{imp}} < 1/(2n_{\text{th}} + 1)$, which is the well-understood requirement on the measurement sensitivity to feedback-cool a velocity-damped oscillator to its motional ground state [14,41].

In marked contrast, for a structurally damped oscillator that is actively stiffened, the apparent initial occupation (i.e., before feedback damping has commenced) in Eq. (22), $n_{\text{th,eff}} + n_{\text{ba}} + n_{\text{imp}}(\Omega_{\text{eff}}/\Gamma_0[\Omega_{\text{eff}}])^2$, has a thermal component (first term), $n_{\text{th,eff}} = n_{\text{th}}[\Omega_0](\Omega_0/\Omega_{\text{eff}})$, that decreases with increasing spring frequency—a form of thermal noise dilution [39,40]—and an additional term (third term), $n_{\text{imp}}(\Omega_{\text{eff}}/\Gamma_0[\Omega_{\text{eff}}])^2 = n_{\text{imp}}(\Omega_{\text{eff}}^2/\Gamma_0\Omega_0)^2$, that increases with the spring frequency—a form of feedback back-action arising from imprecision noise fed back as a force noise in realizing the active spring. The opposing scaling of these two effects

with the spring frequency, with the former scaling as Ω_{eff}^{-1} and the latter as Ω_{eff}^4 , implies an optimal value of the spring frequency beyond which the dilution of thermal noise is nullified by increase in feedback back-action from the spring. For a given measurement imprecision (which is independent from the effective frequency for the structurally damped oscillator)

$$n_{\text{imp}} = \frac{1}{4\eta Q_0} \left(\frac{\Omega_0}{\Omega_{\text{SQL}}} \right)^2, \quad (23)$$

that optimal spring frequency is given by (for the relevant case, $n_{\text{imp}} \ll 1$),

$$\Omega_{\text{eff,opt}} \approx \Omega_0 \left(\frac{n_{\text{th}}[\Omega_0]}{n_{\text{imp}}} \frac{1}{4Q_0^2} \right)^{1/5} \quad (24)$$

$$= \Omega_0 \left(\frac{\eta n_{\text{th}}}{Q_0} \right)^{1/5} \left(\frac{\Omega_{\text{SQL}}}{\Omega_0} \right)^{2/5}, \quad (25)$$

where $Q_0 \equiv \Omega_0/\Gamma_0[\Omega_0]$ is the intrinsic quality factor of the oscillator. Inserting this back into Eq. (22) gives

$$\begin{aligned} n_{\text{eff}} + \frac{1}{2} &\approx \left(\frac{5}{28/5} (n_{\text{th}}^2 Q_0)^{2/5} n_{\text{imp}}^{1/5} + n_{\text{ba}} + \frac{1}{2} \right) \frac{\Gamma_0[\Omega_{\text{eff}}]}{\Gamma_{\text{eff}}} \\ &\quad + n_{\text{imp}} \frac{\Gamma_{\text{eff}}}{\Gamma_0[\Omega_{\text{eff}}]} \\ &\geq 2 \sqrt{\left(\frac{5}{28/5} (n_{\text{th}}^2 Q_0)^{2/5} n_{\text{imp}}^{1/5} + n_{\text{ba}} + \frac{1}{2} \right) n_{\text{imp}}} \\ &\geq 2 \sqrt{\frac{5}{28/5} (n_{\text{th}}^2 Q_0 n_{\text{imp}}^3)^{2/5} + \frac{1}{16}}. \end{aligned}$$

Here the second line is the result of optimizing over the feedback damping rate Γ_{eff} , while the last line is from the uncertainty principle (and we have omitted a small $O(n_{\text{imp}})$ term). In order that $n_{\text{eff}} < 1$, the last equation implies the requirement

$$n_{\text{imp}} < \frac{\sqrt{2}}{5^{5/6} n_{\text{th}}^{-2/3} Q_0^{-1/3}} \quad (26)$$

on the measurement sensitivity. For the experimentally relevant regime where the oscillator begins in a large thermal state, i.e., $n_{\text{th}} \gg 1$, the requirement on the measurement sensitivity is slightly weaker for the case where the oscillator is structurally damped and actively stiffened (scaling as $n_{\text{th}}^{-2/3}$) compared to the case of a velocity-damped oscillator (scaling as n_{th}^{-1}). The condition for n_{imp} in Eq. (26) can be rewritten as that for the mechanical Q value,

$$Q_0 > \left(\frac{5}{8} \right)^{5/4} n_{\text{th}} \left(\frac{\Omega_0}{\Omega_{\text{SQL}}} \right)^3, \quad (27)$$

or in terms of the oft-quoted “ Qf product,” $Q_0 f_0 > (k_B T/h) \times (5/8)^{5/4} (\Omega_0/\Omega_{\text{SQL}})^3$. Note that the necessary condition on the mechanical quality factor is relaxed for a low-frequency oscillator strongly coupled to a quantum-noise-limited optical field (i.e., $\Omega_{\text{SQL}} \gg \Omega_0$). The unique Ω_{SQL}^{-3} scaling on the Q -factor requirement is consistent with the idea that as Ω_{SQL} increases, larger active spring frequencies can be realized; for a structurally damped oscillator, its thermal occupation reduces as Ω_{eff}^{-1} , while the penalty from feedback back-action in realizing the spring worsens as $n_{\text{imp}} \Omega_{\text{eff}}^4 \propto$

$(\Omega_{\text{eff}}^2/\Omega_{\text{SQL}})^2$; their ratio is upper bounded by a factor that scales as Ω_{SQL}^{-3} .

B. General case: Detuned readout with finite-bandwidth feedback

The more general case harnesses the freedom to both detune the readout field from the optical cavity resonance—which produces an optical spring and rotates the quadrature of the outgoing field with respect to the input field—and a variable-quadrature homodyne detection of the outgoing field—which can be sensitive to the quantum correlations developed via the radiation pressure interaction. In this case, for a fixed optomechanical system, an experimenter has control over five parameters: the gain of the feedback filter g_{fb} , which effectively sets the feedback damping rate Γ_{fb} ; the cutoff frequencies Ω_{L} and Ω_{H} , which together with the feedback gain determine the feedback spring frequency Ω_{fb} ; the detuning, which contributes to the radiation pressure-induced spring and damping; and the effective readout phase θ_{eff} .

In the following we will interchangeably use the phonon number and the purity as figures of merit to assess the quality of the quantum state that is realized. The purity satisfies $0 \leq \mu \leq 1$, where the upper (lower) bound corresponds to a maximally pure (mixed) state. In the scenario we consider, where the initial state of the oscillator is Gaussian (specifically, assumed to be thermal), and measurement and feedback are linear in the oscillator’s position, the state realized by feedback is also Gaussian. For Gaussian states, the purity is related to the average quantum number of its thermal component as $\mu^{-1} = 2n_{\text{eff}} + 1$. Thus Eq. (21) directly gives the inverse of the purity. Note, however, that the conventionally employed criteria for having realized the ground state of motion, $n_{\text{eff}} < 1$, corresponds to a purity of $\mu > 1/3$.

For fixed detuning, the dependence of the readout angle is through the imprecision and the imprecision-back-action correlations,

$$n_{\text{imp}} \equiv n_{\text{imp}}^{\theta_{\text{eff}}} = n_{\text{imp}}^{\pi/2} (1 + \cot^2 \theta_{\text{eff}}), \quad (28)$$

$$n_{\text{cor}} \equiv n_{\text{cor}}^{\theta_{\text{eff}}} = n_{\text{cor}}^{\pi/4} \cot \theta_{\text{eff}}, \quad (29)$$

where $n_{\text{imp}}^{\pi/2} = 1/(16\eta n_{\text{ba}})$ is the imprecision for the conventional phase-quadrature readout, and $n_{\text{cor}}^{\pi/4} = 1/(2\sqrt{\eta})$. Clearly, the phase-quadrature readout ($\theta_{\text{eff}} = \pi/2$) minimizes imprecision without harnessing any quantum correlations ($n_{\text{cor}}^{\pi/2} = 0$), while the amplitude-quadrature readout contains no information about the motion (i.e., $n_{\text{imp}}^0 \rightarrow \infty$). In the context of displacement measurement, the trade-off between these two scenarios is the principle of so-called variational measurement that can realize displacement sensitivity better than that by phase-quadrature readout [52–56]. Improved displacement sensitivity, in the context of feedback control, produces less feedback back-action; thus, optimizing the readout angle to harness quantum correlations can lead to better state purity (with other parameters fixed).

Inserting Eq. (28) in Eq. (21), the latter can be put into the form

$$R\mu^{-1} = \frac{C_{\text{tot}}}{g} \left(n_{\text{th,eff}} + n_{\text{ba}} + \frac{1}{2} \right) + gC_{\text{imp}}n_{\text{imp}}^{\pi/2} (1 + \cot^2 \theta) - C_{\text{cor}}n_{\text{cor}}^{\pi/4} \cot \theta, \quad (30)$$

where $g \equiv \Gamma_0[\Omega_{\text{eff}}]/\Gamma_{\text{eff}}$ is the factor by which the damping rate has increased due to feedback, $R \equiv 1 - \Omega_{\text{H}}/\Omega_{\text{L}}$, and $C_{\text{tot,imp,cor}}$ are the dimensionless prefactors for each of the three terms in Eq. (21):

$$\begin{aligned} C_{\text{tot}} &\equiv \frac{2\Omega_{\text{eff}}^2 + (\Omega_{\text{L}} - \Omega_{\text{H}})\Gamma_{\text{eff}} + 2\Omega_{\text{L}}^2}{\Omega_{\text{L}}^2}, \\ C_{\text{imp}} &\equiv \frac{2\Omega_{\text{eff}}^2 + (\Omega_{\text{L}} - \Omega_{\text{H}})\Gamma_{\text{eff}} + 2\Omega_{\text{H}}^2}{\Omega_{\text{eff}}^2}, \\ C_{\text{cor}} &\equiv \frac{2\Omega_{\text{eff}}^2 + (\Omega_{\text{L}} - \Omega_{\text{H}})\Gamma_{\text{eff}} + 2\Omega_{\text{L}}\Omega_{\text{H}}}{\Omega_{\text{L}}\Omega_{\text{eff}}}, \end{aligned} \quad (31)$$

which are themselves functions of g , $\Omega_{\text{H,L}}$. In this sense, the final occupation depends on five parameters: the effective readout angle (which includes the detuning), the increase in damping due to feedback, quantified by g , and the filter cutoff frequencies $\Omega_{\text{H,L}}$; the filter DC gain (g_{fb}) and spring frequency (Ω_{eff}) can be determined in terms of these.

The optimal readout angle is defined to be the one that maximizes the final state purity μ . Completing the square in the angle-dependent terms of Eq. (30),

$$\begin{aligned} R\mu^{-1} &= \frac{C_{\text{tot}}}{g} \left(n_{\text{th,eff}} + n_{\text{ba}} + \frac{1}{2} \right) + gC_{\text{imp}}n_{\text{imp}}^{\pi/2} \\ &+ gC_{\text{imp}}n_{\text{imp}}^{\pi/2} \left[\left(\cot \theta - \frac{C_{\text{cor}}n_{\text{cor}}^{\pi/4}}{2gC_{\text{imp}}n_{\text{imp}}^{\pi/2}} \right)^2 \right. \\ &\left. - \left(\frac{C_{\text{cor}}n_{\text{cor}}^{\pi/4}}{2gC_{\text{imp}}n_{\text{imp}}^{\pi/2}} \right)^2 \right] \\ &\geq \frac{C_{\text{tot}}}{g} \left(n_{\text{th,eff}} + n_{\text{ba}} + \frac{1}{2} - \frac{(C_{\text{cor}}n_{\text{cor}}^{\pi/4})^2}{4C_{\text{tot}}C_{\text{imp}}n_{\text{imp}}^{\pi/2}} \right) \\ &+ gC_{\text{imp}}n_{\text{imp}}^{\pi/2}, \end{aligned} \quad (32)$$

where the inequality is true for the choice $\cot \theta = C_{\text{cor}}n_{\text{cor}}^{\pi/4}/(2gC_{\text{imp}}n_{\text{imp}}^{\pi/2})$, which minimizes the expression in the first line, and dictates the optimal readout angle.

The negative term in the first parentheses of the last inequality above represents the decrease in back-action due to back-action cancellation in variable-quadrature readout. Indeed rewriting the back-action-related part inside those parentheses in the form

$$\begin{aligned} n_{\text{ba}} - \frac{(C_{\text{cor}}n_{\text{cor}}^{\pi/4})^2}{4C_{\text{tot}}C_{\text{imp}}n_{\text{imp}}^{\pi/2}} &= n_{\text{ba}} \left(1 - \frac{(C_{\text{cor}}n_{\text{cor}}^{\pi/4})^2}{4C_{\text{tot}}C_{\text{imp}}n_{\text{ba}}n_{\text{imp}}^{\pi/2}} \right) \\ &\geq n_{\text{ba}} \left(1 - \frac{C_{\text{cor}}^2}{C_{\text{tot}}C_{\text{imp}}} \right) \end{aligned}$$

shows the ideal efficacy of back-action evasion with variable-quadrature readout. (Here the inequality is a result of the statements of the uncertainty principle, $n_{\text{ba}}n_{\text{imp}}^{\pi/2} \geq 1/16$, and

$n_{\text{cor}}^{\pi/4} \leq 1/2$.) Ideally, all back-action is canceled, corresponding to the condition $C_{\text{cor}}^2 = C_{\text{tot}}C_{\text{imp}}$; as it turns out, this happens when [57] $C_{\text{tot}} = 2$. From Eq. (31), and the fact that $\Omega_{\text{H}} < \Omega_{\text{eff}} < \Omega_{\text{L}}$, it follows that $\Omega_{\text{L}} \gtrsim \sqrt{\Omega_{\text{H}}\Gamma_{\text{eff}}/2}$. This further implies that $C_{\text{imp}} \approx 2$.

Thus, in the ideal case where these conditions can be met, all back-action can be suppressed, and so

$$\begin{aligned} \mu^{-1} &\geq \frac{2}{g} \left(n_{\text{th,eff}} + \frac{1}{2} \right) + 2gn_{\text{imp}}^{\pi/2} \\ &\geq 4\sqrt{\left(n_{\text{th,eff}} + \frac{1}{2} \right) n_{\text{imp}}^{\pi/2}}, \end{aligned} \quad (33)$$

indicating that the ground state can be realized if $n_{\text{imp}}^{\pi/2} \lesssim (3/4)^2 n_{\text{th,eff}}^{-1} = (3/4)^2 n_{\text{th}}(\Omega_0/\Omega_{\text{eff}})^2$, for a readout angle $\theta \approx \pi/4$.

The practical benefit of variable-quadrature readout is that for a given measurement imprecision, it can materialize moderate back-action cancellation so that the occupation achieved by feedback damping is lower than if phase readout were employed. To illustrate this practical scenario, we numerically optimize the purity as a function of the five parameters: the two cutoff frequencies (Ω_{L} and Ω_{H}), the feedback gain ($\Gamma_{\text{fb}} \simeq \Gamma_{\text{eff}}$), the normalized detuning (δ), and the readout angle (θ_{eff}). The purity is optimized for varying quantum cooperativities, $C_Q \equiv n_{\text{ba}}/n_{\text{th}}$. In order to emulate conditions of fixed input power, the cutoff frequencies are normalized by the SQL frequency with zero detuning,

$$\Omega_{\text{SQL},0} = \sqrt{1 + \delta^2} \Omega_{\text{SQL}}. \quad (34)$$

For the same reason, we define $C_{Q,\text{SQL}}$ to be the quantum cooperativity at the SQL frequency with zero detuning.

Figure 2 shows the result of numerically optimizing the achievable purity as a function of quantum cooperativity $C_{Q,\text{SQL}}$. Blue lines show the performance of phase quadrature readout ($\theta = \pi/2$), while red shows the case where the readout laser is blue detuned, and the cavity output is subjected to variable-quadrature homodyne measurement. Variable-quadrature readout performs better in terms of the achievable state purity at all values of the cooperativity (a result also known in the context of velocity-damped oscillators [43]). Ground-state cooling, where $\mu > 1/3$, can be achieved at $C_{Q,\text{SQL}} \gtrsim 1$, for a readout angle $\theta \approx \pi/3$. The ultimate purity that can be achieved remains asymptotically bounded by $\mu < \sqrt{\eta}$.

At small cooperativity, the optimal filter cutoff frequencies are relatively high, while the optimal detuning is small. On the other hand, at large cooperativity, the optimal cutoff frequencies are small and the optimal detuning is high. This implies that at small (large) cooperativity, the feedback (optical) spring must be dominant. The reason is that in the small-cooperativity regime, the optomechanical coupling is not strong enough to realize radiation pressure springs large enough to take advantage of the unique scaling of structural thermal noise, whereas in the high-cooperativity regime, the feedback spring introduces additional decoherence from feedback back-action, so that the optical spring is ideal in this regime. In either case, the optimal spring frequency is around the SQL frequency.

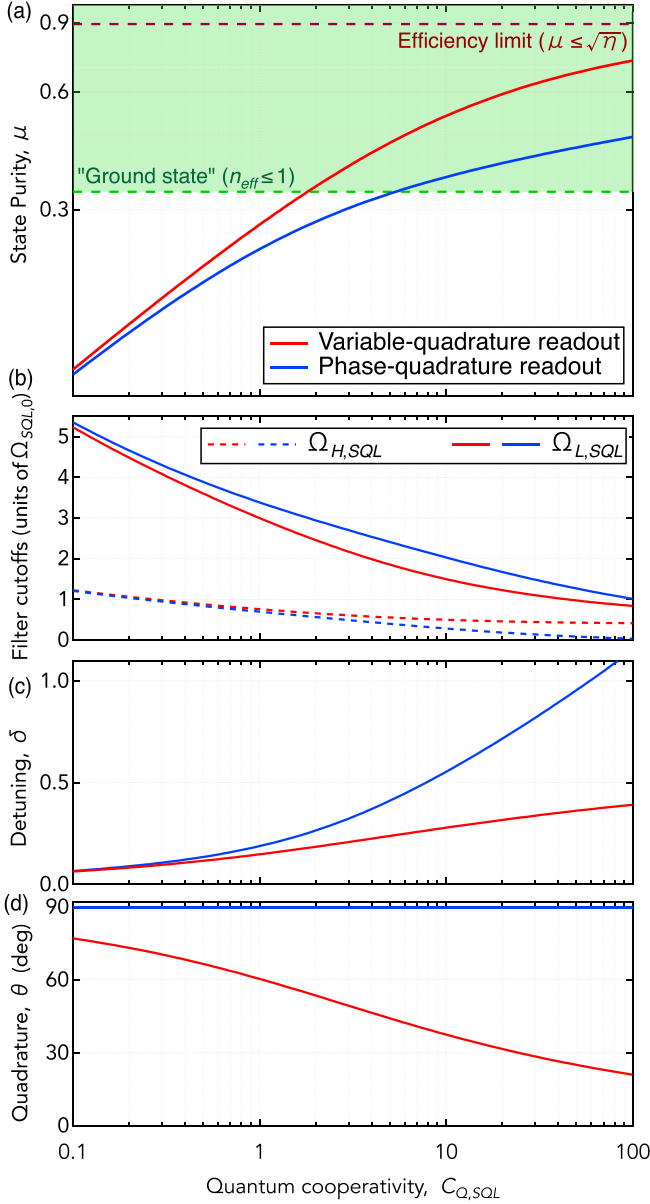


FIG. 2. (a) Maximum achievable purity at any quantum cooperativity with active spring and detuned readout for a structurally damped oscillator. The red (blue) lines correspond to optimized (phase-fixed) readout angle in all panels. The region represents $n_{\text{eff}} < 1$ ($\mu < 1/3$). The brown dotted line indicates the limit to achievable purity due to inefficient detection, i.e., $\mu < \sqrt{\eta}$ ($\eta = 0.8$ here). (b) The feedback filter cutoff frequencies in units of the SQL frequency $\Omega_{\text{SQL},0}$; solid lines are the low-pass cutoff and dashed lines are the high-pass cutoff. (c) The optimal cavity detuning (normalized to FWHM). (d) The optimal readout angle.

IV. CONCLUSION

We have investigated the implications of structural damping on feedback-based motional ground-state preparation of elastically bound macroscopic mechanical oscillators. We find that the requirement to realize the ground state is less stringent compared to the oft-studied case of a velocity-damped oscillator. That is because structural thermal noise reduces with increasing frequency much faster than velocity-proportional

thermal noise. Hence actively stiffening the oscillator mode to take advantage of this decrease can be fruitful. However, that decrease comes at the expense of increasing back-action force fluctuations from the agency that realizes the stiffened spring. The trade-off between these competing sources of decoherence is optimized when the spring frequency is around the SQL frequency. Finally, feedback can be performed using a variable-quadrature homodyne measurement of the oscillator's displacement, which outperforms feedback based on phase-quadrature measurements at all values of the radiation-pressure cooperativity; this is due to back-action cancellation intrinsic to the variable-quadrature measurement scheme.

All of the above conclusions crucially rely on the implicit assumption that the favorable frequency scaling of structural thermal noise continues well beyond the SQL frequency of the mechanical mode of interest. This necessitates careful suspension design to eliminate other mechanical modes in that vicinity.

These observations are directly relevant to experiments that hope to realize pure quantum states of macroscopic mechanical oscillators to explore the interface between quantum physics and gravity.

ACKNOWLEDGMENTS

We thank Hiroaki Ishizuka and Koji Nagano for fruitful discussions. K.K. is supported by JSPS Overseas Research Fellowship.

APPENDIX A: IMPRECISION-BACK-ACTION PRODUCT FOR ARBITRARY DETUNING

In this section, we present the general form of the imprecision-back-action product for the displacement measurement of a mechanical oscillator at arbitrary detuning and homodyne angle.

Let us consider a mechanical oscillator embedded as the end mirror of a single-sided optical cavity, pumped by an ideal coherent state at the effective detuning Δ . The intracavity optical fluctuations (δa) and mechanical displacement fluctuations (δx) are described by the quantum Langevin equations [44]:

$$\delta \dot{a} = \left(i\Delta - \frac{\kappa}{2} \right) \delta a + \sqrt{\kappa} \delta a_{\text{in}} + iG\sqrt{\bar{n}}\delta x, \quad (\text{A1})$$

$$\delta \ddot{x} + \Gamma_m \delta \dot{x} + \Omega_m^2 \delta x = \frac{1}{m} (\delta F_{\text{th}} - \hbar G \sqrt{\bar{n}} (\delta a + \delta a^\dagger)). \quad (\text{A2})$$

Note that Eq. (A1) implies that the entry port is the dominant source of intracavity field losses. We may rewrite these equations in the Fourier domain as

$$\delta a[\Omega] = \frac{\sqrt{\kappa} \delta a_{\text{in}} + iG\sqrt{\bar{n}}\delta x}{-i(\Delta + \Omega) + \kappa/2}, \quad (\text{A3})$$

$$\delta x[\Omega] = \chi_m (\delta F_{\text{th}} + \delta F_{\text{opt}}), \quad (\text{A4})$$

where $\chi_m = (m(\Omega_m^2 - \Omega^2 - i\Omega\Gamma_m))^{-1}$ is the intrinsic susceptibility of the mechanical oscillator, and $\delta F_{\text{opt}} = -\hbar G \sqrt{\bar{n}} (\delta a + \delta a^\dagger)$ is the total back-action force exerted on the mechanical oscillator due to the radiation pressure interaction. The reflected field, given by

$$\delta a_{\text{ref}} = \delta a_{\text{in}} - \sqrt{\kappa} \delta a, \quad (\text{A5})$$

is subjected to ideal homodyne detection with a local oscillator phase shifted by θ ; the resulting photocurrent fluctuations are proportional to fluctuations of the quadrature:

$$\delta q_{\text{ref}}^\theta = \frac{1}{\sqrt{2}}(\delta a_{\text{ref}} e^{-i\theta} + \delta a_{\text{ref}}^\dagger e^{i\theta}). \quad (\text{A6})$$

We may compute the spectral density of the homodyne quadrature as

$$\bar{S}_{qq}^{\theta, \Delta, \text{ref}}[\Omega] 2\pi \delta[0] = \langle \delta q_{\text{ref}}^\theta[\Omega] \delta q_{\text{ref}}^\theta[-\Omega] \rangle, \quad (\text{A7})$$

which may be written as

$$\begin{aligned} \bar{S}_{qq}^{\theta, \Delta, \text{ref}}[\Omega] &\propto \bar{S}_{xx}^{\theta, \Delta, \text{imp}}[\Omega] + |\chi_m|^2 (\bar{S}_{xx}^{\text{th}}[\Omega] + \bar{S}_{FF}^{\delta, \text{rp}}[\Omega]) \\ &+ 2\text{Re}(\chi_m \bar{S}_{Fx}^{\theta, \Delta, \text{rp, imp}}[\Omega]). \end{aligned} \quad (\text{A8})$$

Computing this spectrum from Eq. (A6) following Eq. (A7) and noting the only nonzero correlator for the input vacuum fluctuations, $\langle \delta a_{\text{in}}[\Omega] \delta a_{\text{in}}^\dagger[-\Omega] \rangle = 2\pi \delta[0]$, we can identify the imprecision noise spectral density, $\bar{S}_{xx}^{\theta, \Delta, \text{imp}}$, the back-action force spectral density, $\bar{S}_{FF}^{\delta, \text{rp}}$, as well as the correlation term, $\bar{S}_{Fx}^{\theta, \Delta, \text{rp, imp}}$, as follows.

Defining two frequency scale factors $\delta \equiv \frac{2\Delta}{\kappa}$ and $\omega \equiv \frac{2\Omega}{\kappa}$, the spectral density of the imprecision noise in Eq. (A8) is given by

$$\bar{S}_{xx}^{\theta, \delta, \text{imp}}[\omega] = A^{\text{imp}} \bar{S}_{xx}^{\frac{\pi}{2}, 0, \text{imp}}[\omega], \quad (\text{A9})$$

where

$$A^{\text{imp}} = (1 + \omega^2)^{-1} \frac{(1 + (\delta + \omega)^2)(1 + (\delta - \omega)^2)}{(\sin \theta - \delta \cos \theta)^2 + \omega^2 \sin^2(\theta)}, \quad (\text{A10})$$

$$\bar{S}_{xx}^{\frac{\pi}{2}, 0, \text{imp}}[\omega] = \left(\frac{\kappa}{16G^2\hbar} \right) (1 + \omega^2). \quad (\text{A11})$$

Next, the optical back-action force δF_{rp} is the part of δF_{opt} that only depends on the incoming vacuum field fluctuations, δa_{in} and $\delta a_{\text{in}}^\dagger$. Its symmetrized spectral density as identified in Eq. (A8) is expressed as

$$\bar{S}_{FF}^{\delta, \text{rp}}[\omega] = A^{\text{rp}} \bar{S}_{FF}^{0, \text{rp}}[\omega], \quad (\text{A12})$$

while in the broadband cavity regime ($\Omega \ll \kappa$ or $\omega \ll 1$), it is given by

$$\bar{S}_{Fx}^{\theta, \delta, \text{rp, imp}}[\omega] = -\frac{\hbar}{2}(\cot(\theta - \arctan \delta) + O(\omega)). \quad (\text{A20})$$

Note that in the presence of lossy detection, the correlation term in Eq. (A20) is modified as $[\bar{S}_{Fx}^{\text{rp, imp}}]_\eta = [\bar{S}_{Fx}^{\text{rp, imp}}]_{\eta=1}/\sqrt{\eta}$.

APPENDIX B: CALCULATION OF THE MEAN PHONON NUMBER

Here we describe the details of the integration of the power spectra \bar{S}_{xx} of the oscillator under the combined action of

where

$$A^{\text{rp}} = (1 + \omega^2) \frac{1 + \delta^2 + \omega^2}{(1 + (\delta + \omega)^2)(1 + (\delta - \omega)^2)}, \quad (\text{A13})$$

$$\bar{S}_{FF}^{0, \text{rp}}[\omega] = 4\hbar^2 \frac{G^2 \bar{n}}{\kappa} (1 + \omega^2)^{-1}. \quad (\text{A14})$$

Hence, the imprecision-back-action product in the general case of an arbitrary effective detuning and homodyne measurement angle is given by

$$\bar{S}_{xx}^{\theta, \delta, \text{imp}}[\omega] \bar{S}_{FF}^{\delta, \text{rp}}[\omega] = \frac{\hbar^2}{4} \frac{1 + \delta^2 + \omega^2}{(\sin \theta - \delta \cos \theta)^2 + \omega^2 \sin^2(\theta)}. \quad (\text{A15})$$

Note that the minimum value of the product is precisely $\hbar^2/4$, for $\delta = 0$ and $\theta = \pi/2$; i.e., resonant readout of the phase quadrature is ideal.

In the broadband cavity regime (i.e., $\Omega \ll \kappa$ or $\omega \ll 1$), we have that

$$\bar{S}_{xx}^{\theta, \delta, \text{imp}}[\omega] \approx \bar{S}_{xx}^{\frac{\pi}{2}, 0, \text{imp}}[\omega \ll 1] \left(\frac{1 + \delta^2}{\sin^2(\theta - \arctan \delta)} + O(\omega^2) \right), \quad (\text{A16})$$

$$\bar{S}_{FF}^{\delta, \text{rp}}[\omega] \approx \bar{S}_{FF}^{0, \text{rp}}[\omega \ll 1] \left(\frac{1}{1 + \delta^2} + O(\omega^2) \right), \quad (\text{A17})$$

and, therefore,

$$\bar{S}_{xx}^{\theta, \delta, \text{imp}}[\omega] \bar{S}_{FF}^{\delta, \text{rp}}[\omega] \approx \frac{\hbar^2}{4} \csc^2(\theta - \arctan \delta), \quad (\text{A18})$$

i.e., the effect of detuning, on the imprecision-back-action product in the broadband cavity regime, is equivalent to a quadrature rotation $\arctan(2\Delta/\kappa)$ by the cavity. Furthermore, in the limit of $\delta, \omega \ll 1$, measuring the phase quadrature ($\theta = \pi/2$) is indeed the optimal strategy.

In the case of lossy homodyne detection, quantified by a nonunit detection efficiency $\eta \leq 1$, the imprecision-back-action product is modified as $[\bar{S}_{xx}^{\text{imp}} \bar{S}_{FF}^{\text{rp}}]_\eta = [\bar{S}_{xx}^{\text{imp}} \bar{S}_{FF}^{\text{rp}}]_{\eta=1}/\eta$. Thus, the effect of detuning and general readout quadrature in Eq. (A18) can be interpreted as an effective loss, $\sin^2(\theta - \arctan \alpha)$.

Lastly, Eq. (A8) allows us to identify the cross-correlation spectral density between the back-action force and the imprecision noise. In general, it is given by

$$\bar{S}_{Fx}^{\theta, \delta, \text{rp, imp}}[\omega] = -\frac{\hbar}{2} \frac{(\cos \theta + \delta \sin \theta)(\sin \theta - \delta \cos \theta) + \omega^2 \sin \theta \cos \theta - i\omega \delta}{(\sin \theta - \delta \cos \theta)^2 + \omega^2 \sin^2 \theta} \quad (\text{A19})$$

feedback and detuned optical spring. Using the feedback filter in Eq. (20), Eq. (18) takes the form

$$\begin{aligned} \bar{S}_{xx}[\Omega] &= |\chi_{\text{eff}}[\Omega]|^2 \left[\left(1 + \frac{1}{C_Q[\Omega_{\text{eff}}]} \right) \bar{S}_{FF}^{\text{rp}} \right. \\ &+ \left(\frac{m\Omega_0^2 \Omega_L}{\Omega_H} \right)^2 \frac{\Omega^2 + \Omega_H^2}{\Omega^2 + \Omega_L^2} g_{\text{fb}}^2 \bar{S}_{xx}^{\text{imp}} \\ &\left. + \frac{2m\Omega_0^2 \Omega_L}{\Omega_H} \frac{\Omega^2 + \Omega_H \Omega_L}{\Omega^2 + \Omega_L^2} g_{\text{fb}} \bar{S}_{Fx}^{\text{rp, imp}} \right], \end{aligned} \quad (\text{B1})$$

where $C_Q[\Omega_{\text{eff}}] = \bar{S}_{FF}^{\text{rp}}/S_{FF}^{\text{th}}[\Omega_{\text{eff}}]$ is the quantum cooperativity. Considering that the typical feedback damping is dominant in the total effective damping ($\Gamma_{\text{eff}} \simeq \Gamma_{\text{fb}}$), this can be recast as

$$(\Omega^2 + \Omega_L^2)|\chi_{\text{eff}}[\Omega]|^{-2}\bar{S}_{xx}[\Omega] = \Lambda_L\Omega^2 + \Lambda_H\Omega_L^2, \quad (\text{B2})$$

where

$$\Lambda_L = \left(1 + \frac{1}{C_Q[\Omega_{\text{eff}}]}\right)\bar{S}_{FF}^{\text{rp}} + m^2\Omega_L^2\Gamma_{\text{eff}}^2\bar{S}_{xx}^{\text{imp}} + 2m\Omega_L\Gamma_{\text{eff}}\bar{S}_{Fx}^{\text{rp,imp}}, \quad (\text{B3})$$

$$\Lambda_H = \left(1 + \frac{1}{C_Q[\Omega_{\text{eff}}]}\right)\bar{S}_{FF}^{\text{rp}} + m^2\Omega_H^2\Gamma_{\text{eff}}^2\bar{S}_{xx}^{\text{imp}} + 2m\Omega_H\Gamma_{\text{eff}}\bar{S}_{Fx}^{\text{rp,imp}}. \quad (\text{B4})$$

The inverse of the effective susceptibility is represented as

$$\frac{\Omega_L + i\Omega}{m}\chi_{\text{eff}}^{-1}[\Omega] = -i\Omega^3 - s_1\Omega^2 + is_2\Omega + \Omega_L\Omega_{\text{eff}}^2, \quad (\text{B5})$$

where

$$s_1 = \Omega_L + \Gamma_0 + \Gamma_{\text{rp}}, \quad (\text{B6})$$

$$s_2 = \Omega_{\text{eff}}^2 + (\Omega_L - \Omega_H)\Gamma_{\text{eff}}, \quad (\text{B7})$$

and $\Omega_{\text{eff}}^2 = \Omega_0^2 + \Omega_{\text{rp}}^2 + \Omega_H\Gamma_{\text{fb}}$. In order to calculate the integration in Eq. (19), we use the following identity (see Eq. 3.112 of [58]):

$$\int_{-\infty}^{\infty} dx \frac{g_n(x)}{h_n(x)h_n(-x)} = (-1)^{n+1} \frac{\pi i M_n}{a_0 \Delta_n}, \quad (\text{B8})$$

where

$$g_n(x) = b_0x^{2n-2} + b_1x^{2n-4} + \dots + b_{n-1}, \quad (\text{B9})$$

$$h_n(x) = a_0x^n + a_1x^{n-1} + \dots + a_n, \quad (\text{B10})$$

$$\Delta_n = \begin{vmatrix} a_1 & a_3 & a_5 & \dots & 0 \\ a_0 & a_2 & a_4 & & 0 \\ 0 & a_1 & a_3 & & 0 \\ \vdots & & & \ddots & \\ 0 & 0 & 0 & & a_n \end{vmatrix}, \quad (\text{B11})$$

$$M_n = \begin{vmatrix} b_0 & b_1 & b_2 & \dots & b_{n-1} \\ a_0 & a_2 & a_4 & & 0 \\ 0 & a_1 & a_3 & & 0 \\ \vdots & & & \ddots & \\ 0 & 0 & 0 & & a_n \end{vmatrix}. \quad (\text{B12})$$

Working to first order in Ω/κ (since we assume the system is in the broadband cavity regime), this identity can be applied with $n = 3$. Here,

$$\Delta_3 = a_3(a_1a_2 - a_0a_3), \quad (\text{B13})$$

$$M_3 = b_0a_2a_3 - b_1a_0a_3 + b_2a_0a_1. \quad (\text{B14})$$

We use

$$\begin{cases} a_0 = 1 \\ a_1 = s_1 \\ a_2 = s_2 \\ a_3 = \Omega_L\Omega_{\text{eff}}^2 \end{cases}, \quad \begin{cases} b_0 = 0 \\ b_1 = \Lambda_L \\ b_2 = -\Lambda_H\Omega_L^2 \end{cases}, \quad (\text{B15})$$

to calculate $\langle \delta x^2 \rangle$, and

$$\begin{cases} a_0 = 1 \\ a_1 = s_1 \\ a_2 = s_2 \\ a_3 = \Omega_L\Omega_{\text{eff}}^2 \end{cases}, \quad \begin{cases} b_0 = -\Lambda_L \\ b_1 = \Lambda_H\Omega_L^2 \\ b_2 = 0 \end{cases}, \quad (\text{B16})$$

to calculate $\langle \delta p^2 \rangle$, respectively. The integrals are performed as

$$\langle \delta x^2 \rangle = \frac{1}{2m^2\Omega_{\text{eff}}^2} \frac{\Lambda_L\Omega_{\text{eff}}^2 + \Lambda_H\Omega_Ls_1}{s_1s_2 - \Omega_L\Omega_{\text{eff}}^2}, \quad (\text{B17})$$

$$\langle \delta p^2 \rangle = \frac{1}{2} \frac{\Lambda_Ls_2 + \Lambda_H\Omega_L^2}{s_1s_2 - \Omega_L\Omega_{\text{eff}}^2}. \quad (\text{B18})$$

Typically we choose the low-pass cutoff frequency of the filter which is much larger than the optical dissipation, so $s_1 \simeq \Omega_L$. Thus, the inverse of the purity is given by

$$\mu^{-1} = \frac{\Lambda_L(\Omega_{\text{eff}}^2 + s_2) + 2\Lambda_H\Omega_L^2}{2\hbar m\Omega_{\text{eff}}\Omega_L(s_2 - \Omega_{\text{eff}}^2)}, \quad (\text{B19})$$

which is the result in Eq. (21).

- [1] C. Whittle, E. D. Hall, S. Dwyer, N. Mavalvala, V. Sudhir, and LIGO Instrument Science Group, *Science* **372**, 1333 (2021).
 [2] L. Neuhaus, R. Metzdrorff, S. Zerkani, S. Chua, J. Teissier, D. Garcia-Sanchez, S. Deleglise, T. Jacqmin, T. Briant, J. Degallaix, V. Dolique, G. Cagnoli, O. L. Traon, C. Chartier, A. Heidmann, and P.-F. Cohadon, [arXiv:2104.11648](https://arxiv.org/abs/2104.11648).
 [3] A. Vinante, M. Bionotto, M. Bonaldi, M. Cerdonio, L. Conti, P. Falferi, N. Liguori, S. Longo, R. Mezzena, A.

- Ortolan, G. A. Prodi, F. Salemi, L. Taffarello, G. Vedovato, S. Vitale, and J.-P. Zendri, *Phys. Rev. Lett.* **101**, 033601 (2008).
 [4] F. Diedrich, J. C. Bergquist, W. M. Itano, and D. J. Wineland, *Phys. Rev. Lett.* **62**, 403 (1989).
 [5] C. Monroe, D. M. Meekhof, B. E. King, S. R. Jefferts, W. M. Itano, D. J. Wineland, and P. Gould, *Phys. Rev. Lett.* **75**, 4011 (1995).

- [6] H. Perrin, A. Kuhn, I. Bouchoule, and C. Salomon, *Europhys. Lett.* **42**, 395 (1998).
- [7] J. Eschner, G. Morigi, F. Schmidt-Kaler, and R. Blatt, *J. Opt. Soc. Am. B* **20**, 1003 (2003).
- [8] P. Maunz, T. Puppe, I. Schuster, N. Syassen, P. W. H. Pinkse, and G. Rempe, *Nature (London)* **428**, 50 (2004).
- [9] A. D. Boozer, A. Boca, R. Miller, T. E. Northup, and H. J. Kimble, *Phys. Rev. Lett.* **97**, 083602 (2006).
- [10] J. Chan, T. P. M. Alegre, A. H. Safavi-Naeini, J. T. Hill, A. Krause, S. Gröblacher, M. Aspelmeyer, and O. Painter, *Nature (London)* **478**, 89 (2011).
- [11] J. D. Teufel, T. Donner, D. Li, J. W. Harlow, M. S. Allman, K. Cicak, A. J. Sirois, J. D. Whittaker, K. W. Lehnert, and R. W. Simmonds, *Nature (London)* **475**, 359 (2011).
- [12] A. M. Kaufman, B. J. Lester, and C. A. Regal, *Phys. Rev. X* **2**, 041014 (2012).
- [13] R. W. Peterson, T. P. Purdy, N. S. Kampel, R. W. Andrews, P.-L. Yu, K. W. Lehnert, and C. A. Regal, *Phys. Rev. Lett.* **116**, 063601 (2016).
- [14] M. Rossi, D. Mason, J. Chen, Y. Tsaturyan, and A. Schliesser, *Nature (London)* **563**, 53 (2018).
- [15] U. Delić, M. Reisenbauer, K. Dare, D. Grass, V. Vuletić, N. Kiesel, and M. Aspelmeyer, *Science* **367**, 892 (2020).
- [16] F. Tebbenjohanns, M. Frimmer, V. Jain, D. Windey, and L. Novotny, *Phys. Rev. Lett.* **124**, 013603 (2020).
- [17] L. Magrini, P. Rosenzweig, C. Bach, A. Deutschmann-Olek, S. G. Hofer, S. Hong, N. Kiesel, A. Kugi, and M. Aspelmeyer, *Nature (London)* **595**, 373 (2021).
- [18] F. Tebbenjohanns, M. L. Mattana, M. Rossi, M. Frimmer, and L. Novotny, *Nature (London)* **595**, 378 (2021).
- [19] J. Millen, T. Deesuwana, P. Barker, and J. Anders, *Nat. Nanotechnol.* **9**, 425 (2014).
- [20] S. A. Fedorov, V. Sudhir, R. Schilling, H. Schütz, D. J. Wilson, and T. J. Kippenberg, *Phys. Lett. A* **382**, 2251 (2018), special issue in memory of Professor V. B. Braginsky.
- [21] S. Mancini, D. Vitali, and P. Tombesi, *Phys. Rev. Lett.* **80**, 688 (1998).
- [22] F. Marquardt, J. P. Chen, A. A. Clerk, and S. M. Girvin, *Phys. Rev. Lett.* **99**, 093902 (2007).
- [23] I. Wilson-Rae, N. Nooshi, W. Zwerger, and T. J. Kippenberg, *Phys. Rev. Lett.* **99**, 093901 (2007).
- [24] K. R. Brown, J. Britton, R. J. Epstein, J. Chiaverini, D. Leibfried, and D. J. Wineland, *Phys. Rev. Lett.* **99**, 137205 (2007).
- [25] C. Genes, D. Vitali, P. Tombesi, S. Gigan, and M. Aspelmeyer, *Phys. Rev. A* **77**, 033804 (2008).
- [26] F. Elste, S. M. Girvin, and A. A. Clerk, *Phys. Rev. Lett.* **102**, 207209 (2009).
- [27] X. Wang, S. Vinjanampathy, F. W. Strauch, and K. Jacobs, *Phys. Rev. Lett.* **107**, 177204 (2011).
- [28] A. Xuereb, R. Schnabel, and K. Hammerer, *Phys. Rev. Lett.* **107**, 213604 (2011).
- [29] A. Sawadsky, H. Kaufer, R. M. Nia, S. P. Tarabrin, F. Y. Khalili, K. Hammerer, and R. Schnabel, *Phys. Rev. Lett.* **114**, 043601 (2015).
- [30] X. Xu, T. Purdy, and J. M. Taylor, *Phys. Rev. Lett.* **118**, 223602 (2017).
- [31] C. Sommer and C. Genes, *Phys. Rev. Lett.* **123**, 203605 (2019).
- [32] H.-K. Lau and A. A. Clerk, *Phys. Rev. Lett.* **124**, 103602 (2020).
- [33] R. Christian, *Vacuum* **16**, 175 (1966).
- [34] S. A. Beresnev, V. G. Chernyak, and G. A. Fomyagin, *J. Fluid Mech.* **219**, 405 (1990).
- [35] A. Cavalleri, G. Ciani, R. Dolesi, M. Hueller, D. Nicolodi, D. Tombolato, S. Vitale, P. J. Wass, and W. J. Weber, *Phys. Lett. A* **374**, 3365 (2010).
- [36] P. R. Saulson, *Phys. Rev. D* **42**, 2437 (1990).
- [37] J. Cripe, N. Aggarwal, R. Lanza, A. Libson, R. Singh, P. Heu, D. Follman, G. D. Cole, N. Mavalvala, and T. Corbitt, *Nature (London)* **568**, 364 (2019).
- [38] V. B. Braginsky, M. L. Gorodetsky, and F. Y. Khalili, *Phys. Lett. A* **232**, 340 (1997).
- [39] T. Corbitt, C. Wipf, T. Bodiya, D. Ottaway, D. Sigg, N. Smith, S. Whitcomb, and N. Mavalvala, *Phys. Rev. Lett.* **99**, 160801 (2007).
- [40] K.-K. Ni, R. Norte, D. J. Wilson, J. D. Hood, D. E. Chang, O. Painter, and H. J. Kimble, *Phys. Rev. Lett.* **108**, 214302 (2012).
- [41] D. J. Wilson, V. Sudhir, N. Piro, R. Schilling, A. Ghadimi, and T. J. Kippenberg, *Nature (London)* **524**, 325 (2015).
- [42] V. B. Braginsky and S. P. Vyatchanin, *Phys. Lett. A* **293**, 228 (2002).
- [43] H. Habibi, E. Zeuthen, M. Ghanaatshoar, and K. Hammerer, *J. Opt.* **18**, 084004 (2016).
- [44] M. Aspelmeyer, T. J. Kippenberg, and F. Marquardt, *Rev. Mod. Phys.* **86**, 1391 (2014).
- [45] T. Botter, D. W. C. Brooks, N. Brahm, S. Schreppler, and D. M. Stamper-Kurn, *Phys. Rev. A* **85**, 013812 (2012).
- [46] V. B. Braginsky and F. Y. Khalili, in *Quantum Measurement*, edited by K. S. Thorne (Cambridge University Press, Cambridge, UK, 1992).
- [47] A. A. Clerk, M. H. Devoret, S. M. Girvin, F. Marquardt, and R. J. Schoelkopf, *Rev. Mod. Phys.* **82**, 1155 (2010).
- [48] F. K. Du Pré, *Phys. Rev.* **78**, 615 (1950).
- [49] B. Mandelbrot and J. V. Ness, *SIAM Rev.* **10**, 422 (1968).
- [50] M. Nelkin and A. M. S. Tremblay, *J. Stat. Phys.* **25**, 253 (1981).
- [51] D. Vitali, S. Mancini, L. Ribichini, and P. Tombesi, *J. Opt. Soc. Am. B* **20**, 1054 (2003).
- [52] V. Sudhir, R. Schilling, S. A. Fedorov, H. Schütz, D. J. Wilson, and T. J. Kippenberg, *Phys. Rev. X* **7**, 031055 (2017).
- [53] N. S. Kampel, R. W. Peterson, R. Fischer, P.-L. Yu, K. Cicak, R. W. Simmonds, K. W. Lehnert, and C. A. Regal, *Phys. Rev. X* **7**, 021008 (2017).
- [54] D. Mason, J. Chen, M. Rossi, Y. Tsaturyan, and A. Schliesser, *Nat. Phys.* **15**, 745 (2019).
- [55] S. P. Vyatchanin and E. A. Zubova, *Phys. Lett. A* **201**, 269 (1995).
- [56] H. J. Kimble, Y. Levin, A. B. Matsko, K. S. Thorne, and S. P. Vyatchanin, *Phys. Rev. D* **65**, 022002 (2001).
- [57] In order to see how this works out, it is essential to observe that $C_{\text{tot,imp,cor}}$ are constrained: $C_{\text{cor}}^2 / (2C_{\text{imp}}) = \frac{1 + (C_{\text{tot}} - 2)(\Omega_L / \Omega_H)^2}{1 + \frac{1}{2}(C_{\text{tot}} - 2)(\Omega_L / \Omega_H)^2}$. Then, $1 - C_{\text{cor}}^2 / (C_{\text{tot}} C_{\text{imp}}) \propto C_{\text{tot}} - 2$.
- [58] I. S. Gradshteyn and I. M. Ryzhik, *Table of Integrals, Series and Products* (Academic Press, Orlando, FL, 1980), p. 253.